Optical spectroscopy of Pr^{3+} ions in $LiNbO_3$

A. Lorenzo, L.E. Bausá, and J. García Solé
Departamento de Física de Materiales, Universidad Autónoma de Madrid, Cantoblanco, 28049 Madrid, Spain
(Received 3 February 1995)

The optical absorption and fluorescence of Pr^{3+} ion in $LiNbO_3$ has been systematically investigated. This system is characterized by a very intense red emission at 620 nm corresponding to the $^1D_2 \rightarrow {}^3H_4$ transition. The luminescence of the metastable $^3P_0$ state is almost completely quenched in contrast with other materials. The nonradiative deexcitation has been analyzed for the $^1D_2$ multiplet in terms of a multiphonon process, and a quantum efficiency of 0.87 is experimentally deduced for this state at room temperature. Fluorescence quenching of $^1D_2$ is observed when concentration is increased, and a cross-relaxation process is proposed for concentrations above 0.09 mol%. The fluorescence decay time functions are well explained in the frame of the Inokuti and Hirayama model considering mainly an electric dipole-dipole interaction. It has been also concluded that praseodymium ions are randomly distributed in the $LiNbO_3$ host, so that local charge compensating $Pr(Li^+)$-$Pr(Nb^{5+})$ pairs must be disregarded.

I. INTRODUCTION

The present demand of small and compact solid state lasers has supported the use of lithium niobate ($LiNbO_3$) as a laser host crystal. In fact the electro-optic, acousto-optic, and nonlinear properties of this crystal have permitted the development of $LiNbO_3$:MgO:Nd minilasers,[1] which present several interesting functions for laser applications in integrated optics, such as self-frequency doubling, self-Q-switch, and self-mode-locking.[2] This fact together with the advanced technology in the fabrication of $LiNbO_3$ waveguides have intensified the interest in the optical properties of rare earth ions as potential laser active centers in this nonlinear host crystal. The optical bands for a variety of rare earth ions have been studied and reported for this matrix.[3–7] However, for the case of Pr^{3+} ions, only preliminary information has been reported by the authors.[8]

Pr^{3+} ion offers very interesting perspectives as activator ion because of its rich optical spectrum, which extends from the ultraviolet (UV) to the near infrared (IR).[9] In principle, this provides many possibilities for pumping and lasing in several regions of the electromagnetic spectrum, taking into account the large number of excitation and deexcitation channels. In fact, laser action has been demonstrated for a variety of Pr^{3+} doped materials.[11,12]

In this work, the absorption and fluorescence spectra of Pr^{3+} in $LiNbO_3$ are reported in the range from the UV to near IR. The time dependence of the main emission $^1D_2 \rightarrow {}^3H_4$ is investigated as a function of both temperature and concentration, and some conclusions about the mechanisms responsible for the nonradiative relaxation of the $^1D_2$ state can be drawn.

Energy transfer between Pr^{3+} ions has been observed to occur when concentration increases. There have been many reports on energy transfer of Pr^{3+} in several matrices, due to its role in luminescence quenching of the $^1D_2$ and $^3P_0$ states.[13–16] A variety of models have been proposed to account for this phenomenon, some of them based on the continuum model of Inokuti and Hirayama[17] and the other invoking the discrete nature of the crystals. In our case, decay curves are well explained in the frame of the continuum Inokuti and Hirayama model.

II. EXPERIMENTAL DETAILS

Crystals of $LiNbO_3$:Pr^{3+} were grown in our laboratory by the ballance controlled Czochralski technique, from grade I Johnson-Matthey powder, containing several Pr_2O_3 concentrations relative to Nb^{5+} ions in the congruent melt ([Li]/[Nb] = 0.945). The content of Pr^{3+} in the crystal was analyzed by total x-ray fluorescence for only one of the studied samples, and the others were calibrated by means of their optical absorption spectra ranging from 0.04 to 0.57 mol%. The plates were cut and oriented using x-ray diffraction patterns in order to obtain samples with the ferroelectric c axis parallel or perpendicular to the faces and to perform polarized spectra. Absorption spectra were made in the visible and near infrared regions with a Cary 17 spectrophotometer to cover the region 200–2000 nm and a Hitachi U-3501 spectrophotometer in the region 2000–3200 nm.

The luminescence spectra were obtained by using a Xe lamp or a multiline Argon laser as excitation sources. An air cooled Hamamatsu R-928 S photomultiplier or a silicon photodiode were used for the detection. The spectra were corrected by the response of these components. Time dependence of the luminescence was performed using the third harmonic of a pulsed Nd:YAG (yttrium aluminum garnet) laser at 355 nm. The signals were detected with a multialkali photon counter photocathode using gated techniques.

III. ABSORPTION AND FLUORESCENCE

Figure 1 shows the room temperature (RT) absorption spectrum of LiNbO:Pr^{3+} (0.04 mol%), obtained in the range 400–3200 nm for the unpolarized α configuration, i.e., beam parallel to the crystallographic c axis. It consists of several bands corresponding to transitions between the $^3H_4$ ground state and the excited multiplets belonging to the $4f^2$ configuration of the trivalent praseodymium ion. The structure observed inside each band is mainly due to the the Stark splitting of the different multiplets by the effect of the matrix crystal field. As for other rare earth ions, it is expected that Pr^{3+} ion enters the $LiNbO_3$ lattice replacing Li^+ or Nb^{5+} sites. Both sites have C_3 local symmetry so that each state splits into a number of Stark levels depending on its J value.[18] In this sense, recent Rutherford backscattering spectrometry (RBS) experiments have suggested that Pr^{3+} ions replace only Li^+ ions in this host.[19] Additional structure in the spectra can occur due to the presence of Pr^{3+} multicentres in the $LiNbO_3$ matrix, as previously reported by site selective luminescence measurements.[8]

Relative to the nature of the transitions involved in the absorption spectrum of Pr^{3+} ions in $LiNbO_3$, polarized spectra have been taken in different configurations: σ and π spectra (electric component of the electromagnetic field perpendicular and parallel to the crystallographic c axis, respectively). At this point, it is important to mention that the σ-polarized spectrum is quite similar to the α spectrum, revealing a dominant electric dipole character for all the transitions, forced by the noninversion C_3 local symmetry.

An energy level diagram showing the positions of the J states of Pr^{3+} ion in $LiNbO_3$ is displayed in Fig. 2. The thickness (shadowed region) of each state indicates the extent of the crystalline Stark splitting. This diagram, constructed from the absorption and fluorescence data reported in this work, is helpful to label the different transitions involved. Only the $^1S_0$ and the $^1I_6$ states are absent from the scheme, the first one for being too high (about 46 500 cm^{-1})[20] and the second one because the spin-forbidden $^3H_4 \rightarrow {}^1I_6$ transition is masked by the spin-allowed $^3H_4 \rightarrow {}^3P_J$ $(J = 0, 1, 2)$.

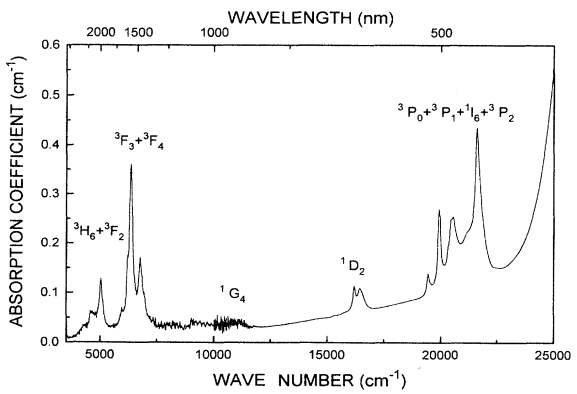

FIG. 1. Absorption spectrum at room temperature of $LiNbO_3$:Pr^{3+} (0.04 mol%).

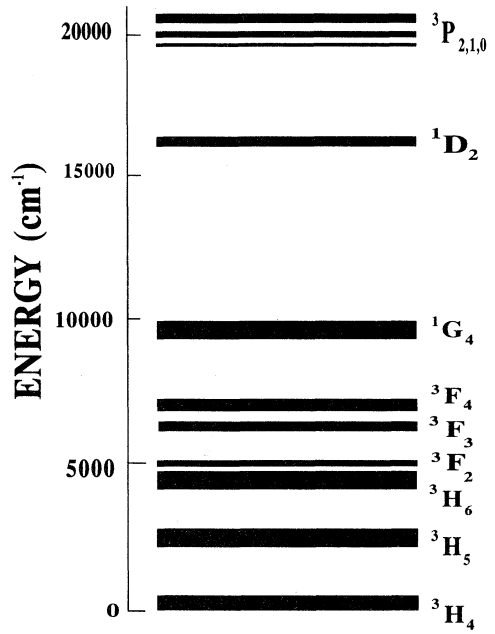

FIG. 2. Scheme of energy levels of $LiNbO_3$:Pr^{3+}.

Figure 3 shows the RT excitation and emission spectra of $LiNbO_3$:Pr^{3+} (0.04 mol%) in the wavelength range from 300 to 1200 nm. The emission spectrum consists of four structured bands centered around 620 nm, 710 nm, 885 nm, and 1050 nm. The excitation spectrum (dotted line) displays three bands at 360 nm, 480 nm, and 610 nm. The latter two bands coincide in energy with the absorption transitions $^3H_4 \rightarrow {}^3P_J$ $(J = 0, 1, 2)$ and $^3H_4 \rightarrow {}^1D_2$, respectively, and are easily identified.

Relative to the broadband appearing in the excitation spectra at 360 nm, it cannot be assigned to any $4f \rightarrow 4f$ intraconfigurational transition, since it is too broad and is located far from any $4f$ state (the $^1S_0$ state should be much more higher).[20] In principle, it could be identified as an interconfigurational $4f \rightarrow 5d$ transition, but there are some features that make this asignment unprobable.

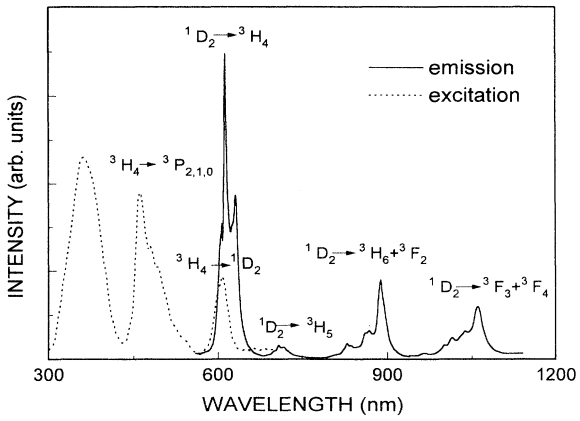

FIG. 3. Emission and excitation spectra of $LiNbO_3$:Pr^{3+} (0.04 mol%) at room temperature. $\lambda_{exc} = 360$ nm; $\lambda_{em} = 715$ nm.

For instance, the position of these states has been reported to be at higher energy in other matrices, around 250 nm.[9,10] Unfortunately, the analysis of this band cannot be properly performed in the absorption spectrum because it overlaps with the absorption edge and contributes to its anomalous raising at 25 000 cm^{-1} (see Fig. 1), which does not correspond to the fundamental absorption edge of $LiNbO_3$. However, a systematic study in the absorption edge region deserves special attention and it is not the aim of this work. Further experiments are now underway to give a definitive assignment to this excitation band.

The excitation spectrum does not change when monitoring any of the emissions in Fig. 3, so that the $^3H_4 \rightarrow {}^1D_2$ absorption is always present. In addition, the same fluorescence spectrum is obtained exciting into the $^1D_2$ or the ^3P_J multiplets. These two facts indicate that the emissions correspond to deexcitations from the $^1D_2$ multiplets to the $^3H_4$, $^3H_5$, $^3H_6+{}^3F_2$, and $^3F_3+{}^3F_4$ multiplets, respectively. The $^1D_2 \rightarrow {}^3H_4$ emission is clearly dominant and produces a very intense red color.

It is important to point out that, at variance with other Pr^{3+} doped oxides,[11,14] in $LiNbO_3$:Pr^{3+}, the main channel of radiative deexcitation is through the $^1D_2$ state instead of the $^3P_0$ state. Luminescence from the ^3P_J is extremely weak even at low temperature and only an emission band peaking at 515 nm and associated to the $^3P_0 \rightarrow {}^3H_4$ transition was detected. Thus, any excitation into levels above $^1D_2$ is followed by a quick nonradiative relaxation to this multiplet, from which several transitions can be seen, the $^1D_2 \rightarrow {}^3H_4$ being the most intense. This was true for all the concentration range studied in this work.

IV. FLUORESCENCE DYNAMICS

In order to deeply understand the luminescence behavior of Pr^{3+} ion in $LiNbO_3$, the time evolution of the luminescence from the emitting levels has been investigated. At this point, another difference must be remarked on concerning the emission behavior of Pr^{3+} ions. The obtained fluorescence lifetime values in our samples are quite different to those obtained for this ion in other matrices. Table I shows the values of the lifetime of $^1D_2$ and $^3P_0$ levels for the case of Pr^{3+} in a variety of host matrices. In our case, the lifetimes, for the $^1D_2$ and $^3P_0$ states are 33 μs and 0.45 μs, respectively (both values referred to the less concentrated sample, 0.04 mol% at low temperature), which are significantly shorter compared with other systems doped with a similar level of active impurity and for the same temperature. To obtain more information, a study of the fluorescence dynamics has been performed, studying the effect of temperature and Pr^{3+} concentration on the fluorescence decays.

A. Temperature dependence

For the study of the temperature dependence of the fluorescence lifetimes, the less concentrated sample (0.04 mol%), in which all the fluorescence decay times had an exponential shape, has been chosen to avoid concentration effects. As above mentioned, a lifetime of 0.45 μs was obtained at a low temperature for the $^3P_0$ state. However, the temperature dependence of $^3P_0$ fluorescence could not be performed due to the fast quenching observed when temperature increases. Hence, this section will concern the time evolution of the $^1D_2$ state.

TABLE I. Comparison of lifetimes for the Pr^{3+} ion in different matrices.

Matrix	T (K)	$\tau(^1D_2)$	$\tau(^3P_0)$	Ref.
YAG(0.12%)	300	180	8.4	7
YAG(0.12%)	77	260	12.3	7
YAG(1%)	300	55	8	8
YAG(1%)	77		10.2	9
YGG(1%)	4.2		17–19	10
YGG(20%)	4.2		13–15	10
GGG(1%)	4.2		15	11
KYPO(3%)	4.4	180		12
YLF(0.1%)	300	365		13
YLF(0.1%)	77	820		13
YLF(1%)	300	251	50	13
YLF(1%)	13	635	50	13
YLF(0.24%)	4.4		38	14
ZBLA	300	55	15	15
$LaCl_3$(1%)	4.2		14.7	16
$LaBr_3$(1%)	4.2		12	16
SBA(94%)	300	365–470	9–12	17
SBA(94%)	10	700–815	12–15	17
$LiNbO_3$(0.04%)	15	38	0.45	This work
$LiNbO_3$(0.04%)	300	33		This work

Measurements of fluorescence decay times from the $^1D_2$ multiplet have been carried out for temperatures from 15 to 300 K. Pure exponential curves were observed in all the range of temperatures. Lifetimes varied from 38 μs at 15 K to 33 μs at room temperature. Thus, a nonradiative temperature-dependent process is taking place.

The first mechanism to be invoked is multiphonon relaxation to the next lower multiplet, $^1G_4$ (see Fig. 2). These two states are separated by an average distance of 6625 cm^{-1}, which might be reached by the emision of several effective phonons. The phonon spectrum of $LiNbO_3$ presents its maximum energy peak at 880 cm^{-1}, as reported by Claus and Winter.[21] Assuming that this is the effective phonon involved in multiphonon processes, seven of these phonons of maximun energy must be created to release the energy difference between the two states.

Following Moos[22] and Weber,[23] the probability of a nonradiative multiphonon relaxation involving a number p of effective phonons depends on temperature according to

$$W_{\rm nr}^{p}(T) = W_{\rm nr}^{p}(0)\cdot(1+n_{\rm eff})^{p} \ , \tag{1}$$

where $n_{\rm eff}$ is the occupancy of the effective phonon modes,

$$n_{\rm eff} = [\exp(\hbar\omega_{\rm eff}/kT) - 1]^{-1} . \tag{2}$$

Now, the total transition probability of the $^1D_2$ state $W = 1/\tau$ can be expressed as the sum of a radiative plus a nonradiative temperature-dependent contribution,

$$W = W_r + W_{nr}(T). \quad (3)$$

Dividing this expression by the total probability at 0 K, $W(0)$, we obtain

$$W(T) = [W(0) - W_r] \cdot (1 + n_{eff})^p + W_r, \quad (4)$$

which gives us the inverse of the experimental lifetime as a function of temperature. If we plot $1/\tau$ against $(1 + n_{eff})^p$ and assume that $p = 7$, we should obtain a straight line if the multiphonon assumptions are correct. In addition, this fitting will give as a result the values of W_r and $W(0)$ and, hence, $W_{nr}(0)$. Figure 4 shows this plot, where it can be observed that, at very low temperatures, no variation with temperature is obtained and the multiphonon process is not noticeable. When temperature increases, nonradiative relaxation becomes more important and changes can be well fitted by Eq. (1). According to that, multiphonon relaxation with seven effective phonons of 880 cm^{-1} can account for the temperature dependence of the fluorescence decay from the $^1D_2$ multiplet. From this model, the nonradiative and radiative probability associated with the depopulation of $^1D_2$ multiplet can be obtained. At $T = 0$ K the resulting nonradiative probablility, $W_{nr}(0)$, is 925 s^{-1}.

On the other hand, from the value of the raditive probability, W_r, and the experimental lifetimes (38 μs at 15 K and 33 μs at 300 K) an experimental value of nearly 1 can be obtained for the quantum efficiency of the $^1D_2$ state at 15 K, while at 300 K this value is 0.87.

Concerning the $^3P_0$ quantum efficiency, we must point out that a small value according to the almost nonradiative character of this state is expectable. Only the $^3P_0 \rightarrow {}^3H_4$ transition can hardly be observed at low temperatures. The mechanism responsible for this fact can be a multiphonon relaxation, because just four phonons are needed to complete the energy gap to the $^1D_2$ multiplet.

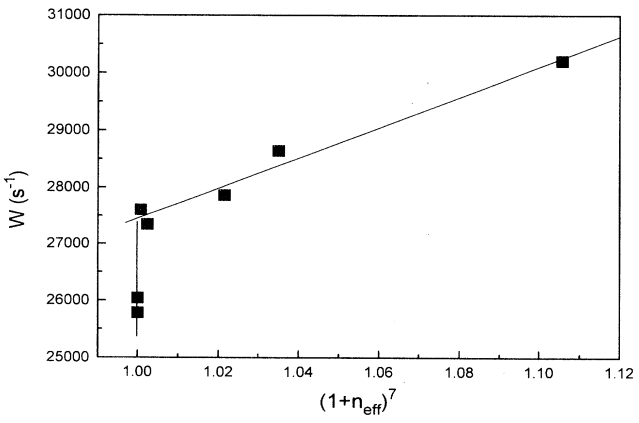

FIG. 4. Fitting to a straight line of the total transition probability of the $^1D_2$ state in $LiNbO_3$:Pr^{3+} (0.04 mol%) according to Eq. (4). The first two points show that at low temperatures, thermal processes are not activated.

In the case of the $^3P_0$ level, quantum efficiency can be experimentally estimated making use of the room temperature absorption and excitation spectra. The efficiency of $^3P_0$ is then given as a function of $^1D_2$ quantum efficiency. Comparing the number of quanta of light absorbed by the ^3P_J and the $^1D_2$ states (estimated by dividing the area under the absorption spectrum by the average wavelength) with the same magnitude in the excitation spectrum and assuming that the only way to nonradiatively depopulate the ^3P_J states is multiphonon relaxation to $^1D_2$, a value of 0.13 is obtained for the $^3P_0$ quantum efficiency.

Finally, other possible ways for a nonradiative depopulation of $^1D_2$ and $^3P_0$ states have to be considered. In this sense, we have to say that the up-conversion process or excited state absorption have to be disregarded as far as the excitation power was not high enough and no dependence of lifetime with exciting power was observed.

On the other hand, energy transfer or diffusion between Pr^{3+} ions could also account for this nonradiative temperature-dependent process. However, luminescence decays observed from $^1D_2$ were purely exponential, thus showing not relevant energy transfer at this concentration level. There could be some other transfer mechanism, such as fast diffusion, which gave us pure exponential decays, but, in our case, this is not very probable due to the low concentration of the sample and also because nonexponenciality starts at much higher concentrations, as will be shown in the next section.

B. Effect of concentration

In order to gain additional information on the luminescence properties of Pr^{3+} ions in $LiNbO_3$, the fluorescence dynamics of the $^1D_2$ emitting state were investigated as a function of Pr^{3+} concentration. Decay curves for all concentrations were obtained for the intense $^1D_2 \rightarrow {}^3H_4$ transition at about 620 nm after pulsed excitation at 355 nm. For concentrations higher than 0.2 mol% nonexponential decays were obtained and decay time values became shorter with increasing Pr^{3+} doping level. Figure 5 displays the low temperature decays for three samples with different Pr^{3+} content.

This variation of fluorescence with concentration indicates energy transfer processes. As has been demonstrated for other Pr doped systems,[13] the model proposed in our case is a resonant cross-relaxation mechanism involving two identical Pr^{3+} ions (donor and acceptor), according to the following scheme:

$$[^1D_2, {}^3H_4] \rightarrow [^1G_4, {}^3F_4] \ .$$

In fact, the case in which the dominant mechanism is a fast energy diffusion has to be neglected. This transfer process can be present when impurity concentration is high and, in this case, the excitation moves from donor to donor for some time before being transferred to an acceptor or a trap where the process ends up. If this were the dominant mechanism, pure exponential decays

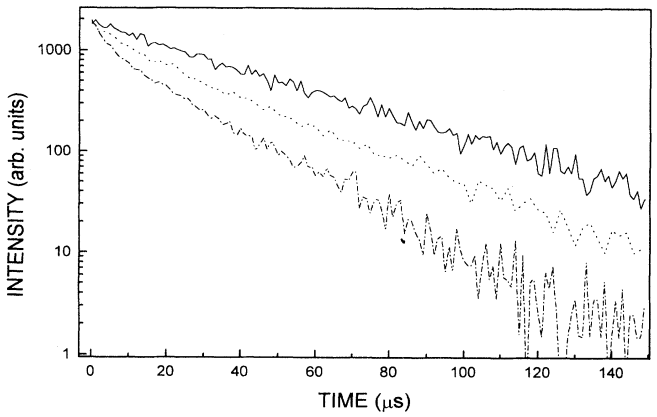

FIG. 5. Fluorescence decay time curves for the $^1D_2 \rightarrow {}^3H_4$, for different Pr^{3+} concentrations at 15 K. Solid line: 0.04 mol%; dotted line: 0.27 mol%; dotted dashed line: 0.57 mol%.

should be obtained. As far as our decays are markedly nonexponential, fast diffusion is rejected. However, difussion processes could be competitive with a direct transfer at sufficiently high concentrations and, as a consequence, the tail of the decay curve will show an exponential behavior with a characteristic time τ given by

$$\frac{1}{\tau} = \frac{1}{\tau_0} + \frac{1}{\tau_D} , \tag{5}$$

where τ_D is the probability of the diffusion process.[24] Hereafter, we define as donors all the Pr^{3+} ions in the excited $^1D_2$ levels, and as acceptors all surrounding Pr^{3+} ions in the ground state.

In our case, we can asume that concentrations are weak enough to neglect the probability of formation of new crystalline phases or clusters and no evidence on this has been reported for other rare earth doped $LiNbO_3$ crystals. In addition, the possibility of local charge compensating $Pr(Li^+)$-$Pr(Nb^{5+})$ pairs has to be disregarded as far as Pr^{3+} ions only enter Li^+ positions, as reported by RBS experiments.[19] Thus, the natural physical model we consider is that in which both, sensitizing and activator impurity ions, are arranged randomly on the suitable lattice sites of the crystal.

On the other hand, there are several models to explain a direct transfer (cross-relaxation) mechanism. Some of them take into account the discrete crystal structure and consider the real distances where each neighbor acceptor can be placed.[13] However, for the present, we begin to consider in our case the continuum model of Inokuti and Hirayama,[17] in which the probability of finding an acceptor in a sphere of radius R around the donor is

$$n(R) = N 4\pi R^2 dR , \tag{6}$$

where N is the ion concentration.

Assuming electrostatic multipole interaction, the energy transfer probability can be expressed in general by

$$W(R) = \frac{1}{\tau_0}\left(\frac{R_0}{R}\right)^s , \tag{7}$$

where R_0 is the critical radius defined as the distance at which an isolated donor-acceptor pair has the same transfer rate as the spontaneous decay rate of the donor, τ_0. The parameter s is a number equal to 6, 8, or 10 depending on whether the transfer mechanism is electric dipole-dipole, dipole-quadrupole, or quadrupole-quadrupole, respectively. With this transfer probability, Inokuti and Hirayama arrived to the following expression for the intensity decay:

$$I(t) = I(0)\exp\left\{-\frac{t}{\tau_0} - \Gamma\left(1-\frac{3}{s}\right)\frac{N}{c_0}\cdot\left(\frac{t}{\tau_0}\right)^{3/s}\right\} , \tag{8}$$

in which c_0 is a critical concentration defined as $3/4\pi R_0^3$ and $\Gamma(x)$ is the gamma function evaluated in x.

The character of the mechanism responsible of the transfer can be inferred by plotting $\ln I(t) + t/\tau_0$ against $t^{3/s}$. We should get a straight line for the best value of s. For most of the samples, the best fit obtained is for $s = 6$. Then, the decay functions are fitted to the Inokuti-Hirayama formula setting the critical radius R_0 as a variable parameter. The intrinsic decay time $\tau_0 = 38$ μs is obtained from the low temperature decay of the less concentrated sample, which is purely exponential. The initial value of $s = 6$ is proposed according to the shape of the decays.

Figures 6(a), (b), and (c) show the results of the fitting for $s = 6$, for three Pr^{3+} concentrations. The good agreement of the fittings in the case of the less concentrated samples can be seen. Table II shows the results obtained for the critical radius R_0. As observed, for the less concentrated samples (0.21 and 0.27 mol%), similar values of R_0 (around 1.15 nm) are obtained supporting the consistency of the model proposed.

On the other hand, as shown in Fig. 6(a) the fitting is not very good for the most concentrated sample, finding a significant deviation for long times. In order to solve this deviation, the contribution of a diffusion process has been considered according to Eq. (5). However, this produced the effect of a shortening in the decay at long times, which is the opposite of what is needed in our case [see Fig. 6(a)].

Another mechanism should then be found to account for this misfit. If the concentration is increased, the nearest neighbor distance is shorter and higher order processes have to be considered.[13] This seems to be what happens in our system: contributions of dipole-quadrupole processes $s = 8$ become important when concentration increases. In fact, the plot $\ln I(t) + t/\tau_0$ against $t^{3/s}$ is also good for $s = 8$ for the most concentrated sample, indicating an important contribution of short range interactions (R^{-8}). Thus, a better agreement is now obtained for the most concentrated sample, as can be observed in Fig. 6(d), where a fit of Inokuti-Hirayama model with $s = 8$ is applied. In fact, the actual process must be thought of as a combination of two independent processes dipole-dipole and dipole-quadrupole, each with a relative weight. This is the reason why the value of R_0 obtained from the fitting with $s = 8$ (1.28 nm) is very similar to the one obtained for $s = 6$ (1.23 nm) even when both processes have a different nature.

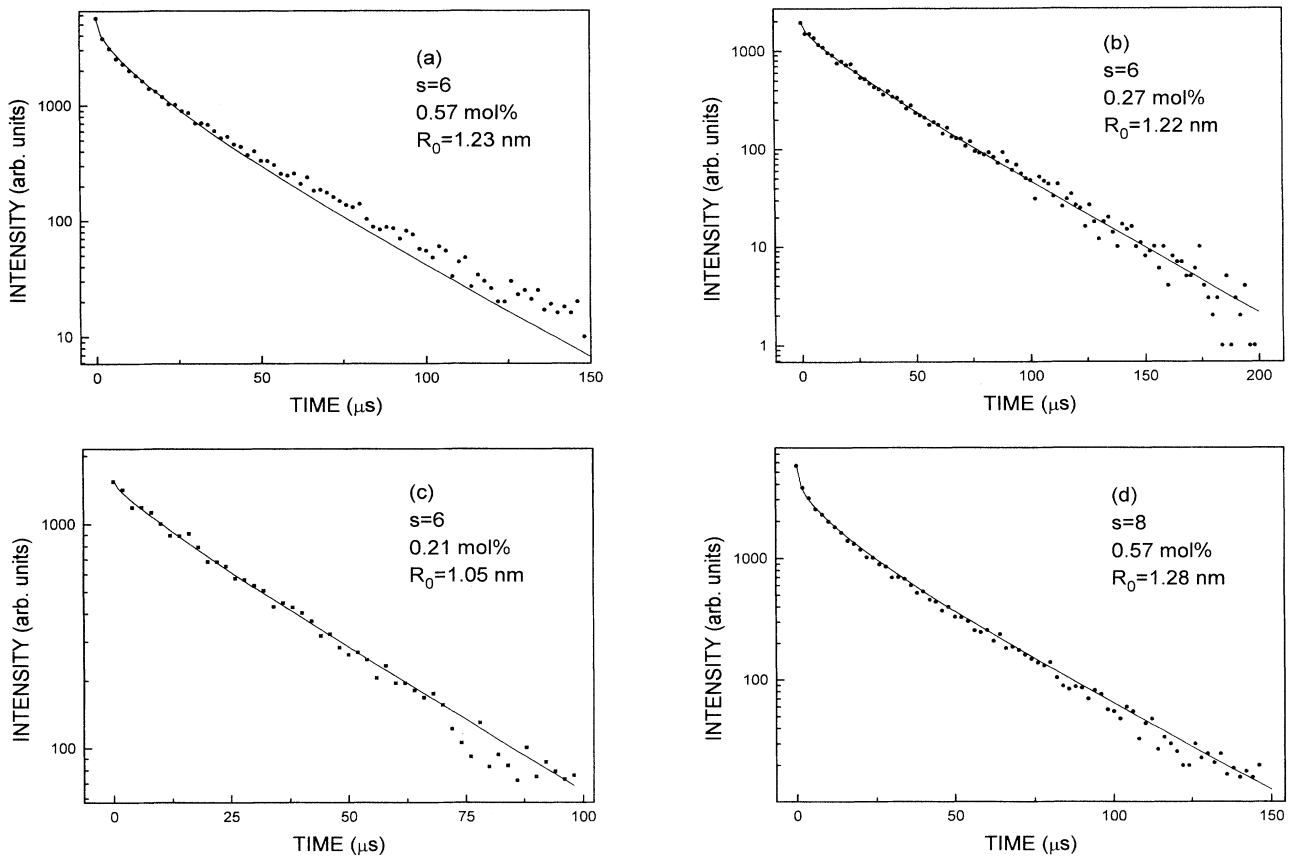

FIG. 6. (a), (b), (c) Fitting of the fluorescence decay time curves to the Inokuti-Hirayama model for three different concentrations considering s=6. (d) Fitting for the most doped sample considering $s = 8$.

The results obtained show the validity of the Inokuti-Hirayama model to explain the fluorescence decay of Pr^{3+} in the $LiNbO_3$ crystal. The direct transfer process between Pr^{3+} ions is well explained in the frame of this continuum model and there is no need to invoke a discrete model. On the other hand, as has been already demonstrated, diffusion processes are not contributing to the energy transfer mechanism in this system.

These results can also be explained in terms of the average Pr-Pr distances, R_{avg}, estimated as $(4\pi N/3)^{-1/3}$, which are shown in Table II. We can justify the absence of diffusion due to the fact that the average distance is of the order of the critical radius R_0 and so it will be very probable to find one acceptor inside the critical radius of a donor, thus making the direct transfer process predominant.

TABLE II. Results of the fitting using the Inokuti-Hirayama model. The last column shows the average Pr-Pr distances estimated from the concentration value.

N (mol%)	N (nm^{-3})	R_0 (nm) $s = 6$	R_0 (nm), $s = 8$	R_{avg} (nm)
0.04	0.0082			3.07
0.21	0.04	1.05	1.13	1.81
0.27	0.05	1.22	1.3	1.68
0.57	0.1028	1.23	1.28	1.32

In addition, we can evaluate the minimum distance from which the overall transfer probability $W^{\infty}_{R_{min}}$ is small compared with intrinsic decay, i.e., 10^{-2} less than $1/\tau_0$.[13] From Eqs. (6) and (7), we can obtain that

$$W^{\infty}_{R_{min}} = \int_{R_{min}}^{\infty} W(R) N 4\pi R dR = \int_{R_{min}}^{\infty} \frac{1}{\tau_0}\left(\frac{R_0}{R}\right)^6 N 4\pi R dR = \frac{4\pi N R_0^6}{3\tau_0 R_{min}^3} \approx 10^{-2}\frac{1}{\tau_0} . \quad (9)$$

From this calculation, a value of $R_{min} = 2.17$ nm is obtained for the less concentrated sample. A comparison with the value of 3.07 nm for the average distance (see Table II) clearly explains the absence of any transfer in this sample.

Once we know the mechanism responsible for the concentration quenching in $LiNbO_3$:Pr^{3+}, we can test the predicted concentration dependence of the nonradiative transfer probability. For dipole-dipole interaction, the transfer probability between two ions at a distance R is given by Eq. (7) with $s = 6$. Then, the average transfer probability of one donor ion in a certain environment can be evaluated by[25]

$$W = \int_V W(R)n(R)dR = N\int_V W(R)4\pi R^2 dR\ . \quad (10)$$

From this expression, a linear concentration dependence is expected when only direct transfer occurs. We first estimate the effective lifetime for the nonexponential decays as the value of t for which $I(t) = I(0)e^{-1}$. According to this the following effective lifetimes, τ_{eff}, are obtained: 38.0, 22.8, 20.2, and 11.0 μs for concentrations of 0.04, 0.21, 0.27, and 0.57 mol%, respectively. Figure 7 shows a plot of the inverse effective lifetime as a function of concentration. The three most doped samples exhibit a linear behavior, thus confirming the direct transfer. On the other hand, the less doped sample remains in the transfer-free zone. From this figure a minimun concentration from which fluorescence quenching of the $^1D_2$ state appears is found to be 0.09 mol%.

Let us now justify the applicability of a continuum model in Pr^{3+} doped $LiNbO_3$. The fluorescence decay of $^1D_2$ state has been analyzed in terms of the energy transfer between Pr^{3+} ions and reconstructed with the Inokuti and Hirayama model. This model assumes that each donor ion in the excited state is surrounded by a random environment of acceptor ions in the ground state. When interaction distances are very short, or the distribution of ion sites cannot be considered as continuum, another model which takes into account the possible positions of the ions in the discrete lattice has to be used.

In the case of $LiNbO_3$, the structure is made of oxygen octahedra in which a Nb^{5+}, a Li^+, and a structural vacancy are alternatingly located according to the following stacking sequence: Nb-Li-vacancy. Recent RBS/channeling experiments ruled out the possibility of double occupancy for Pr^{3+} in $LiNbO_3$ and proposed a substitution of Li^+ ions.[19] Hence, two nearest neighbor Pr^{3+} ions in $LiNbO_3$ should be separated by the minimum Li^+-Li^+ distance, which is 0.397 nm. A "map" of the posible positions of acceptor ions around a donor can be constructed for this crystal. This is depicted in Fig. 8, where the number of available impurity sites, i.e., Li^+ sites, as a function of distance is represented. As can

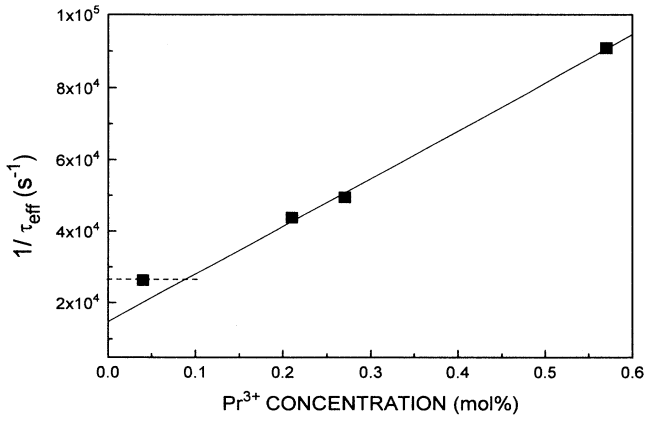

FIG. 7. Inverse of the effective decay time as a function of concentration. The full line shows the fitting according to Eq. (10). The dashed line represents the tranfer-free zone.

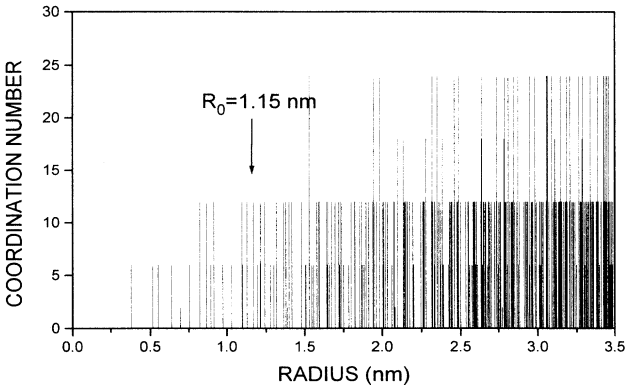

FIG. 8. Distribution of available impurity sites in $LiNbO_3$ around a central Li^+ site.

be seen, at short range, the structure is discrete, but at distances next to the critical radius $R_0 = 1.15$ nm, the structure can be considered continuumlike, which validates the model we used.

Another important point is that the validity of this Inokuti and Hirayama model confirms that the Pr^{3+} ions are homogeneously incorporated in $LiNbO_3$, instead of forming local charge compensating $Pr(Li^+)$-$Pr(Nb^{5+})$ pairs. In fact, if the impurity entered forming any well defined structure breaking the random distribution, the model could not have been applied. Thus, in our case, we can conclude that the Pr^{3+} ions are homogeneously incorporated.

This is an important result if we take into account the crystal structure of $LiNbO_3$. It has been suggested that trivalent rare earths do enter $LiNbO_3$ as pairs subtituting for a Li^+ (2+ excess charge) and its neighbor Nb^{5+} ion (2+ defect charge). In this way, the charge is easily compensated with no need for additional defects. However, as previously mentioned, Pr^{3+} ions have been reported to subtitute for Li^+ ions, while Nb^{5+} and vacant lattice sites have to be disregarded.

This is consistent with our analysis of the decay times using a continuum model, and points out that when impurities are incorporated to $LiNbO_3$, charge compensation is made through the intrinsic lattice defects, i.e., Nb antisites, Li vacancies, without the need of invoking the formation of pairs in the matrix. These defects appear as a consequence of the nonstoichiometry of the matrix (the ratio [Li]/[Nb] not equal to 1).[26,27] A systematic study of the variation of optical properties of Pr^{3+} ions as a function of stoichiometry together with RBS measurements is now going on and will be reported elsewhere.

V. CONCLUSION

In this work, spectroscopic data (absorption and emission) of $LiNbO_3$:Pr^{3+} are presented. Polarized aborption spectra at RT have permitted the construction of the energy levels diagram for Pr^{3+} in this matrix. Emission and excitation spectra clearly show an important difference in the behavior of the main radiative channels of Pr^{3+} in $LiNbO_3$, relative to Pr^{3+} in other systems.

While in most of the matrices, both states $^3P_0$ and $^1D_2$ are equally efficient, in our case, only a very weak luminescence is detected from $^3P_0$ and a strong radiative deexcitation occurs from $^1D_2$. These luminescences have lifetime values of 33 μs for $^1D_2$ and 0.45 μs for $^3P_0$ at room temperature and for very low ion concentrations.

Nonradiative deexcitation of $^1D_2$ can be deduced through the temperature dependence of its exponential lifetime. A multiphonon model is proposed in which seven effective phonons of 880 cm^{-1} must be created to relax the system to the next lower $^1G_4$ state. The temperature evolution provides information about the probability of this process, as well as about the radiative probability. Thus, comparing this radiative probability with experimental lifetimes, quantum efficiencies can be estimated as nearly 1 at low temperature and 0.87 at 300 K. This is in good agreement with the very intense red color observed for the $^1D_2 \rightarrow {}^3H_4$ fluorescence. On the other hand, a value of only 0.13 for the $^3P_0$ quantum efficiency has also been experimentaly estimated.

Fluorescence quenching of the $^1D_2$ state has been demonstrated to occur when the concentration is increased over 0.09 mol%. This is attributed to a cross-relaxation process, the transfer mechanism being dipole-dipole with an important dipole-quadrupole contribution at high concentrations. A continuum distribution of impurity ions has been proved to modelize our system, so that local charge compensating Pr-Pr pairs can be disregarded. Other transfer processes such as diffusion can be rejected.

ACKNOWLEDGMENTS

This paper has been supported by the Comisión Interministerial de Ciencia y Tecnología (CICYT) under Project No. MAT-92/130. The authors wish to acknowledge Servicio Interdepartamental de Apoyo a la Investigación (SIDI) for performing the analysis of Pr^{3+} contents in $LiNbO_3$.

[1] A. Córdova-Plaza, M. Digonnet, and H. J. Shaw, IEEE J. Quantum Electron. **QE-23,** 262 (1987).
[2] E. Lallier, J. P. Pocholle, M. Papuchon, M. de Micheli, J. M. Li, Q. He, D. B. Ostrowski, C. Grezes-Besset, and E. Pelletier, Opt. Lett. **15,** 682 (1990).
[3] A. Lorenzo, L. E. Bausá, and J. Garcia-Solé, J. Phys. Condens. Matter **6,** 1065 (1994).
[4] L. Núñez and F. Cussó, J. Phys. Condens Matter **5,** 5301 (1993).
[5] R. Duchowicz, L. Núñez, J. O. Tocho, and F. Cussó, Solid State Commun. **88,** 439 (1993).
[6] L. Arizmendi and J. M. Cabrera, Phys. Rev. B **31,** 7138 (1985).
[7] H. Loro, M. Voda, F. Jaque, J. García-Solé, and J. E. Muñoz-Santiuste, J. Appl. Phys. **77,** 1 (1995).
[8] A. Lorenzo, L. E. Bausá, M. Voda, and J. García-Solé, J. Phys. (France) IV **4,** C4-381 (1994).
[9] L. R. Elias, W. S. Heaps, and W. M. Yen, Phys. Rev. B **11,** 4989 (1973).
[10] J. Weber, Solid State Commun. **12,** 741 (1973).
[11] M. Malinowski, M. F. Joubert, and B. Jacquier, Phys. Status Solidi A **140,** K49 (1993).
[12] F. Varsanyi, Appl. Phys. Lett. **19,** 169 (1971).
[13] H. Dornauf and J. Heber, J. Lumin. **22,** 1 (1980).
[14] M. Szimanski, J. Lumin. **29,** 467 (1984).
[15] M. Malinowski, J. Phys. Condens. Matter **1,** 4673 (1989).
[16] J. Hegarty, D. L. Huber, and W. M. Yen, Phys Rev. B **25,** 5638 (1982).
[17] M. Inokuti and F. Hirayama, J. Chem. Phys. **43,** 1978 (1965).
[18] B. Henderson and G. P. Imbusch, *Optical Spectroscopy of Inorganic Solids* (Clarendon, Oxford, 1989).
[19] J. García Solé, A. Lorenzo, T. Petit, G. Boulon, B. Roux, and H. Jaffrezic, J. Phys. (France) IV **4,** C4-293 (1994).
[20] R. S. Rana, C. D. Cordero-Montalvo, and N. Bloembergen, J. Chem. Phys. **81,** 2951 (1984).
[21] F. Claus and F. X. Winter, in *Polaritons*, edited by E. Burnstein and F. de Martini (Pergamon, New York, 1972), p. 41.
[22] H. W. Moos, J. Lumin. **1,** 106 (1979).
[23] M. J. Weber, Phys. Rev. B **8,** k54 (1973).
[24] G. P. de Gennes, J. Phys. Chem. Solids **7,** 345 (1958).
[25] F. Auzel, in *Radiationless Processes*, edited by B. Di Bartolo (Plenum, New York, 1980), p. 213.
[26] J. García Solé, Phys. Scr. **T55,** 30 (1994).
[27] B. Macalik, L. E. Bausá, J. García Solé, and F. Jaque, Appl. Phys. Lett. **62,** 1887 (1993).
[28] M. Malinowski, W. Wolinski, R. Wolski, and W. Strek, J. Lumin **48&49,** 235 (1991).
[29] O. Malta, E. Antic-Fidancev, M. Lemaitre-Blaise, J. Dexpert-Ghys, and B. Pirou, Chem. Phys. Lett. **129,** 557 (1986).
[30] E. Antic-Fidancev, M. Lemaitre-Blaise, P. Caro, and J. C. Krupka, Inorg. Chim. Acta **139,** 281 (1987).
[31] E. Antic-Fidancev, M. Lemaitre-Blaise, P. Caro, and J. C. Krupka, J. Less-Common Met. **148,** 167 (1989).
[32] E. Antic-Fidancev, M. Lemaitre-Blaise, P. Porcher, and J. C. Krupka, Eur. J. Solid State Inorg. Chem. **28,** 81 (1991).
[33] J. L. Adam, W. A. Silbey, and D. R. Gabbe, J. Lumin. **33,** 391 (1985).
[34] M. Malinowski, M. F. Joubert, and B. Jacquier, J. Lumin. **60-61,** 179 (1994).
[35] M. Eyal, E. Greenberg, R. Reinsfeld, and N. Spector, Chem. Phys. Lett. **117,** 108 (1985).
[36] K. R. German, A. Kiel, and H. Guggenheim, Phys. Rev. B **11,** 2436 (1975).
[37] G. Mariotto, F. Tietz, E. Zanghellini, and M. Ferrari, J. Lumin. **60-61,** 216 (1994).